Supplementary Information

Selective Heteroepitaxial Synthesis of 2D Bismuth-Based Mixed-Anion Compounds with Interfacial Spin-Orbit Interaction via Atmospheric Solution Routes

Zhengkang Peng,[a] Daichi Oka,*[ab] Yasushi Hirose,[b] and Tomoteru Fukumura[acd]

a. Department of Chemistry, Graduate School of Science, Tohoku University, 6-3 Aramaki Aza Aoba, Aoba, Sendai, Sendai 980-8578, Japan
b. Department of Chemistry, Graduate School of Science, Tokyo Metropolitan University, 1-1 Minami Osawa, Hachioji, Tokyo, 192-0397, Japan
c. WPI Advanced Institute for Materials Research, Tohoku University, Sendai 980-8577, Japan
d. Center for Science and Innovation in Spintronics, Organization for Advanced Studies, Tohoku University, Sendai 980-8577, Japan

Table S1. Temperature and precursors in the synthesis of the Bi_2OS_2 and $Bi_3O_2S_2Cl$ epitaxial thin films.

Product	Temperature (°C)	Precursor 1 (Concentration)	Precursor 2 (Concentration)
Bi_2OS_2	500–530	$BiCl_3$ (3.75 mmol L^{-1}) and thiourea (10 mmol L^{-1})	
$Bi_3O_2S_2Cl$	400–520	$BiCl_3$ (7.5 mmol L^{-1})	thiourea (20 mmol L^{-1})

Table S2. Gas and flow rates in the synthesis of the Bi_2OS_2 and $Bi_3O_2S_2Cl$ epitaxial thin films.

Product	Carrier gas (flow rate) for precursor 1	Dilution gas (flow rate) for precursor 1	Carrier gas (flow rate) for precursor 2	Dilution gas (flow rate) for precursor 2
Bi_2OS_2	N_2 (7.0 L min^{-1})	O_2 (0.1 L min^{-1})	N/A	N/A
$Bi_3O_2S_2Cl$	N_2 (3.5 L min^{-1})	N_2 (0.3 L min^{-1})	N_2 (2.5 L min^{-1})	O_2 (0.2 L min^{-1})

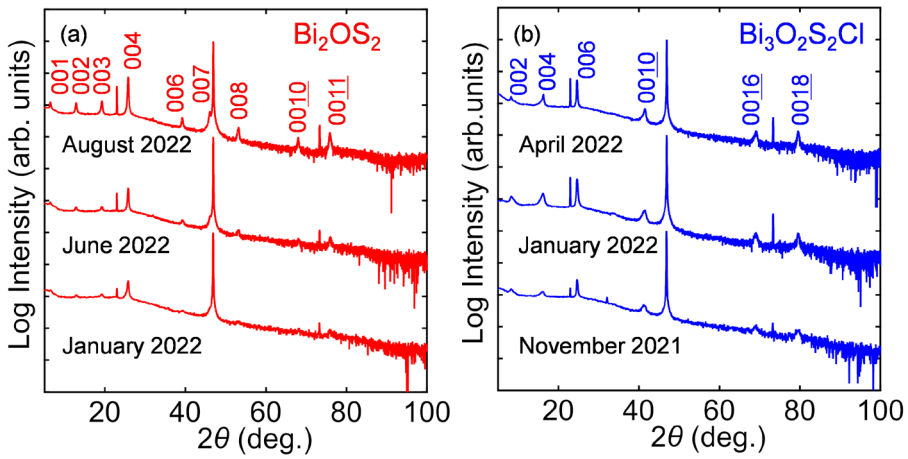

Figure S1. XRD θ–2θ patterns for (a) Bi_2OS_2 and (b) $Bi_3O_2S_2Cl$ thin films synthesized on LSAT (100) substrates in independent experiments on different dates.

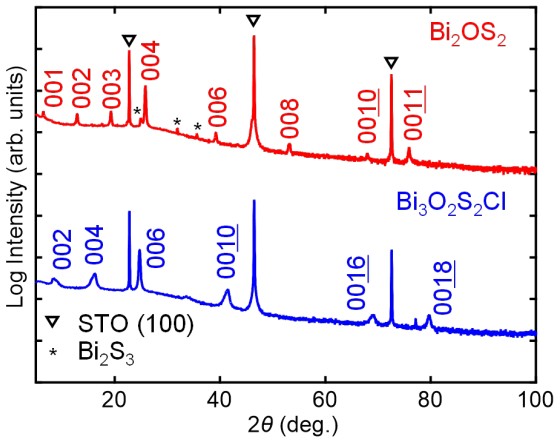

Figure S2. XRD θ–2θ patterns for Bi_2OS_2 and $Bi_3O_2S_2Cl$ epitaxial thin films on $SrTiO_3$ (001) substrates.

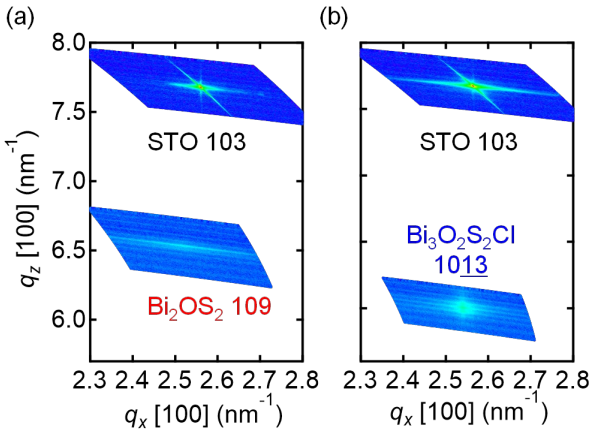

Figure S3. Reciprocal space maps for (a) Bi_2OS_2 and (b) $Bi_3O_2S_2Cl$ epitaxial thin films on $SrTiO_3$ (001) substrates.

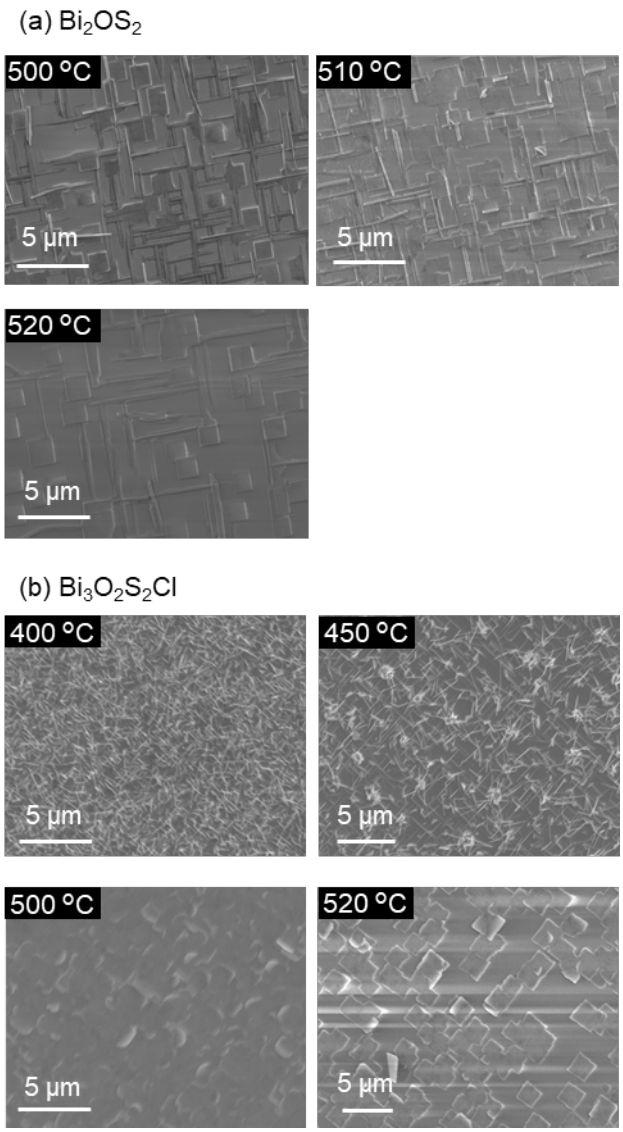

Figure S4. SEM images for a) Bi_2OS_2 and b) $Bi_3O_2S_2Cl$ thin films synthesized on LSAT (001) substrates at various temperatures.

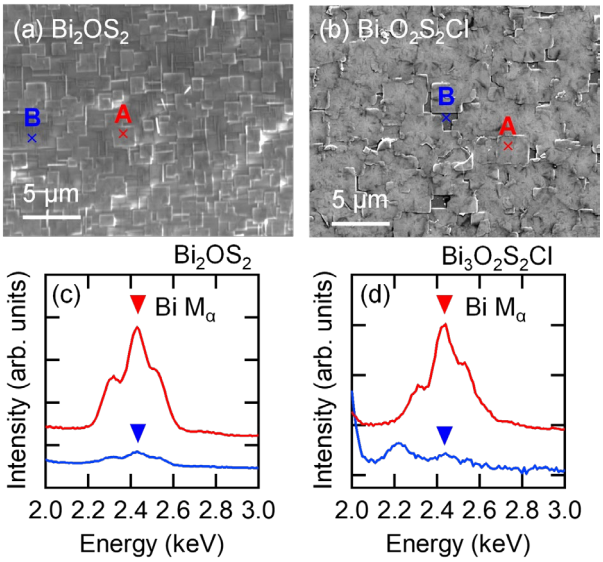

Figure S5. a–b) SEM images and c−d) EDS spectra around the Bi Mα peaks for the spots indicated in (a) and (b) for Bi_2OS_2 (a, c) and $Bi_3O_2S_2Cl$ (b, d) thin films.

Compensation of charge and structural mismatches at the interface between the $Bi_3O_2S_2Cl$ and LSAT substrate

Figure S6a and b shows the crystal structure of δ-Bi_2O_3 with the same fluorite structure as the $[Bi_2O_2]^{2+}$ slab in $Bi_3O_2S_2Cl$ and perovskite-type LSAT. While the Bi^{3+} cation is allocated at the 8 coordinate site in the fluorite structure, La/Sr cations and Al^{3+}/Ta^{5+} cations occupy the 12 and 6 coordinate sites in the perovskite structure, respectively. Thus, the fluorite and perovskite structures cannot be epitaxially stacked without deforming their original structures. In Reference S1, such a structural mismatch was successfully compensated by inserting a buffer layer of defect fluorite $Ln_{0.5}Zr_{0.5}O_{1.75}$ (Ln = La, Nd), where the oxygen defect allows an asymmetric interfacial coordinate structure. Because δ-Bi_2O_3 is also a defect fluorite where 3/4 of the oxygen sites are occupied, formation of a similar interfacial structure is possible. Accordingly, Bi ions would occupy the site close to the A site of the surface layer of the perovskite-type substrate (Figure S6c). This leads to a positively charged interfacial atomic layer of $[BiO]^{1+}$. In order to compensate this charge, formation of δ-Bi_2O_3-like interfacial slab would be favored where occupancy of the oxygen site alternatively varied to form the charged $[Bi_2O_2]^{2+}$ and $[O]^{2-}$ slabs according to the STEM image. The relatively high contrast of the $[O]^{2-}$ slabs in the ABF image suggests partial inclusion of S^{2-} and Cl^{-} ions, although the structure of the δ-Bi_2O_3 layer differs from those of BiOCl and Bi_2O_2S.

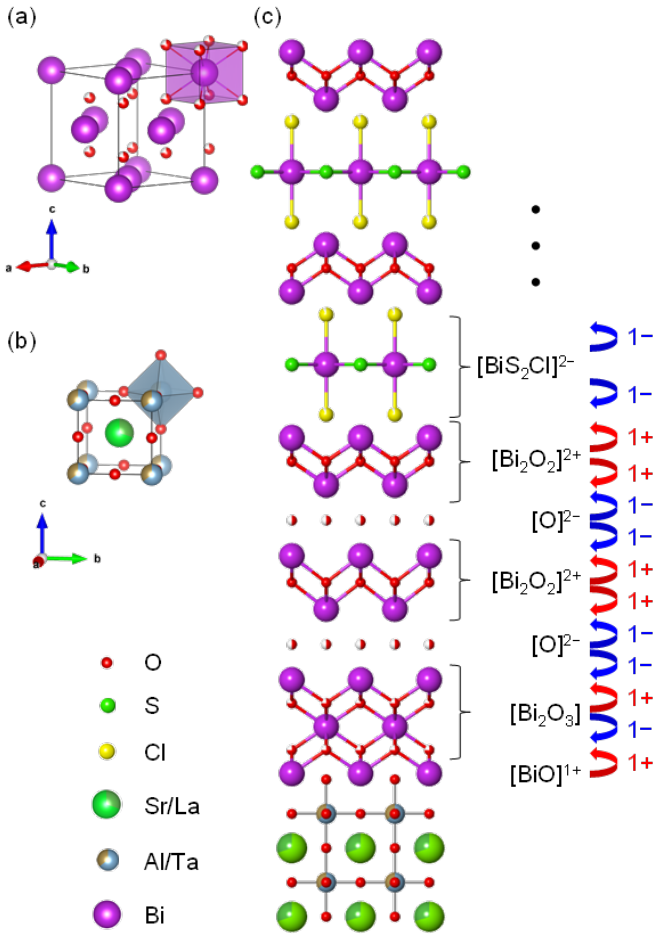

Figure S6. Schematic illustration of the crystal structures of a) fluorite-type δ-Bi_2O_3, b) perovskite-type LSAT, and c) interface between the $Bi_3O_2S_2Cl$ epitaxial thin film and LSAT substrate.

Investigation on the *k*-linear and *k*-cubic SOI in the ILP expression of the weak localization effect

The general formula of the magnetoconductance in the Iordanskii, Lyanda-Geller, Pikus (ILP) theory is given by the following equation: [S2–S4]

$$\Delta G(B) = -\frac{e^2}{2\pi h}\left[\frac{1}{a_0} + \frac{2a_0 + 1 + \frac{B_{SO1}+B_{SO3}}{B}}{a_1\left(a_0 + \frac{B_{SO1}+B_{SO3}}{B}\right) - 2\frac{B_{SO1}}{B}} - \sum_{n=0}^{\infty}\left\{\frac{3}{n} - \frac{3a_n^2 + 2a_n\frac{B_{SO1}+B_{SO3}}{B} - 1 - 2(2n+1)\frac{B_{SO1}}{B}}{\left(a_n + \frac{B_{SO1}+B_{SO3}}{B}\right)a_{n-1}a_{n+1} - 2\frac{B_{SO1}}{B}[(2n+1)a_n - 1]}\right\} + 2ln\frac{B_{tr}}{B} + \Psi\left(\frac{1}{2} + \frac{B_\phi}{B}\right) + 3C\right] \quad \text{(S1)}$$

where e is the elementary charge, h is the Planck constant, C is the Euler constant, $\Psi(x)$ is the digamma function, B_φ and B_{tr} are the characteristic magnetic fields for phase coherence and spin orbit scattering, respectively, B_{SO1} and B_{SO3} are the characteristic magnetic field for spin-orbit scattering derived from the effective Hamiltonian containing the *k*-linear and *k*-cubic terms, respectively, and $a_n = n + \frac{1}{2} + \frac{B_\phi}{B} + \frac{B_{SO1}+B_{SO3}}{B}$. When $B_{SO1} = 0$, equation S1 is simplified to Equation 1 in the main text. Figure S7 is the results of fitting for the magneto conductance data measured for the $Bi_3O_2S_2Cl$ epitaxial thin film at 2 K in the conditions $B_{SO3} = 0$ (with only the *k*-linear term) and $B_{SO1} = 0$ (with only the *k*-cubic term), where the infinite sum was added up to $n = 1 \times 10^5$. While the former model deviated from the experimental data at magnetic fields over ~0.35 T, the latter condition gave reasonable fitting in all the measured range. This situation is similar to the systems with cubic Rashba effect in the previous reports.[S2,S4]

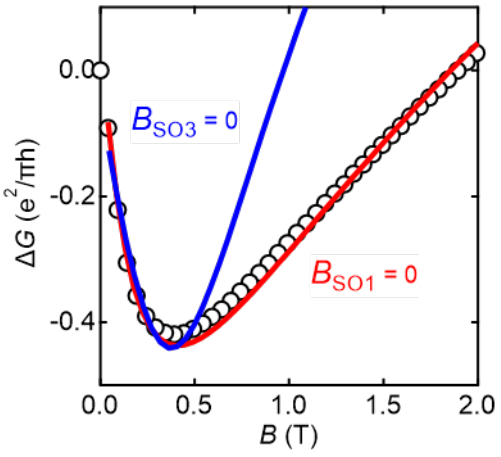

Figure S7. Magnetoconductance for the $Bi_3O_2S_2Cl$ epitaxial thin film under out-of-plane magnetic field at 2 K fitted by equation S1 in the conditions $B_{SO3} = 0$ (with only the *k*-linear term; blue curve) and $B_{SO1} = 0$ (with only the *k*-cubic term; red curve).

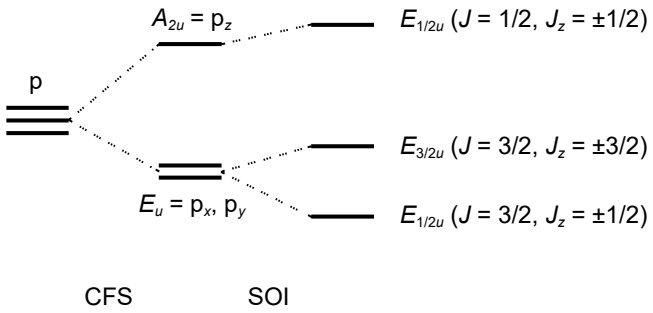

Figure S8. Schematic illustration of the orbital energy level evolution of 6p orbitals of Bi by the crystal field splitting (CFS) under a D_{4h} point group symmetry and spin orbit interaction (SOI).

References

S1 M. O'Sullivan, J. Hadermann, M. Dyer, S. Turner, J. Alaria, T. Manning, A. Abakumov, J. Claridge and M. Rosseinsky, *Nat. Chem.* 2016, **8**, 347–353.

S2 H. Nakamura, T. Koga and T. Kimura, *Phys. Rev. Lett*. 2012, **108**, 206601.

S3 B. L. Altshuler, A. G. Aronov and D. E. Khmelnitsky, J. Phys. C 1982, 15, 7367.

S4 R. Moriya, K. Sawano, Y. Hoshi, S. Masubuchi, Y. Shiraki, A. Wild, C. Neumann, G. Abstreiter, D. Bougeard, T. Koga and T. Machida, *Phys. Rev. Lett*. 2014, **113**, 086601.